



A Neighborhood Impact Driven K-Medoid Clustering and Fuzzy Logic Blended Approach for High Density Impulse Noise Detection and Removal

Aritra Bandyopadhyay¹, Kaustuv Deb², Avishek Chakraborty^{3*}, Atanu Das⁴, Rajib Bag⁵

¹ Department of CSE, Supreme Knowledge Foundation Group of Institutions, Mankundu 712139, India

² Department of Computer Science & Technology, Nalhati Government Polytechnic, Nalhati, Birbhum 731243, India

³ Department of Engineering Science, Academy of Technology, Adisaptagram 712502, India

⁴ Department of MCA, Netaji Subhash Engineering College, Kolkata 700152, India

⁵ Indas Mahavidyalaya, Indas, Bankura 722205, India

Corresponding Author Email: avishek.chakraborty@aot.edu.in

<https://doi.org/10.18280/ts.390532>

ABSTRACT

Received: 30 June 2022

Accepted: 10 October 2022

Keywords:

impulse noise removal, salt and pepper noise, random valued impulse noise, k-medoid clustering, fuzzy logic

In the field of image processing, removing impulse noise has been regarded as one of the most important tasks, primarily because of the noise pattern it presents. Existing filters used the effect of only those non-noisy pixels which were present inside the specified windows ignoring the effect of the non-noisy pixels present in the surrounding windows. So, the least distant non-noisy pixels in the present window as well as in the surrounding windows may have an influence on the present window's noisy pixels. Hence, considering the above factors, in this paper, a two-step technique named KMDCIFF (K-medoid clustering identified fuzzy filter) is proposed for removing impulse noise from digital images. In the proposed KMDCIFF algorithm, the first step is noise detection using K-medoid clustering, followed by a fuzzy logic-acquainted noise reduction strategy that utilizes the least distant local and non-local non-noisy pixels for removal operation. The detection process involves the application of K-medoid clustering on all 5×5 windows produced by centering each pixel of the considered image. In order to remove noise, a 7×7 window is constructed with each detected noisy pixel in the center. Analyzing the impact of the least distant local and non-local pixel on each noisy pixel, the same is replaced by an estimated pixel's intensity value obtained from the most influential non-noisy pixels. KMDCIFF is evaluated using well-known metrics for diverse types of images. At a high noise density of 80%, KMDCIFF exhibited significant peak-signal-to-noise-ratios (PSNRs) of 26.97 dB and 29.67 dB and structural similarity indexes (SSIMs) of 0.8045 and 0.9288 on random and fixed valued impulse noise impacted Lena image, respectively. Comparing the results of the contemporary study to those of previous studies of a similar kind in this sector, the results are unswervingly astounding.

1. INTRODUCTION

In the field of image processing, eliminating impulse noise [1] is a challenging task. Noise may have a significant impact on digital images throughout the collection, transmission, and atmospheric turbulence processes. An erroneous analog-to-digital conversion or an inaccurate memory placement may also lead to noise. Moreover, the presence of noise degrades the quality of the images and impairs subsequent image processing operations, such as compression, morphological processing, segmentation, object identification, and so on. In light of this, image de-noising [2] is a vital step that must be completed in order to pave the way for the subsequent image processing methods. The main goal of this study is to develop a new technique for denoising grayscale images containing impulsive noise patterns. The creation of an 8-bit grayscale image involves assigning intensity values that may land anywhere between 0 and 255 on the defined scale. In general, impulse noise distorts the uniformity of the pixel intensities, causing their values to fluctuate in an unpredictable way. There are two distinct types of impulse noise patterns, which are referred to respectively as fixed-valued impulse noise

(FVIN) [3] and random-valued impulse noise (RVIN) [4]. Fixed value impulse noise is also known as salt and pepper noise because it causes abrupt black and white dots in digital images, with black dots having '0' (minimum) intensity values and white dots having '255' (maximum) intensity values. Black dots are referred to as 'pepper' noise, whereas white dots with maximum intensity values of '255' are referred to as 'salt' noise. These noisy granules with fixed values may be found randomly placed across the images. Edges may also have values as low as 0 and as high as 255, therefore all the '0' and '255' intensity values may not represent noise in their entirety. However, if these intensity levels are abruptly fluctuated from low to high or vice versa, the images seem to be distorted. In contrast to this, RVIN impulse noise generates a wide range of random noise patterns in images owing to its disorderly character. Any grayscale value between 0 and 255, may represent noise in this category. In either case, the noise does not have an effect on all of the pixel's intensities but owing to the arbitrary nature of RVIN, it is difficult to eliminate it in an effective manner. The key issue in this endeavour is to perform the necessary restoration techniques while maintaining the structural integrity of the images. For a

few decades, a variety of non-linear filters were developed to reduce impulsive noise in digital images. The most well-established and extensively used filters for removing impulsive noise are median filters and their modified forms, which have been developed by various authors during all these years. Years of research into the elimination of impulse noise have proven that a filter's success is predicated primarily on the accuracy of its detection mechanism, which must be followed by an equally precise elimination procedure. A variety of improvised median filter variants were developed during the course of the last decade. One of them was the switching median filter, which used detection to separate out noisy pixels from clean ones. The elimination procedure only impacted the noisy pixels, leaving the non-noisy ones untouched by the process. Nair and Mol [5] suggested a switching median filter that operated on a conventional detection approach for filtering out non-noisy pixels. To reconstruct the noisy pixels, either the non-noisy pixels in four directions or the weighted median of the non-noisy pixels in a defined window were used. The primary disadvantage of switching median filters was the degradation in visual fidelity of the produced image brought on by several missed classified pixels. Over the year, another filter by Yuan and Li [6] employed morphological cues paired with dilation to identify the noisy pixels. The modified median filter and the morphological filter were merged into a single approach as part of the removal procedure in order to fix the pixel artefacts brought on by the noise. At varying levels of noise, both switching median filters failed to sustain the filter's efficacy to some extent. In order to solve this problem, adaptive switching median filters have been developed. Thus according to the study of Meher and Singhawat [7], an adaptive switching median filter with variable window size dependent on the availability of non-noisy pixels and a recursive procedure to recover the noisy pixels was recommended. Another filter by Lee et al. [8] exploited the non-noisy pixels in the adaptive-sized neighbourhood to restore noisy pixels and also used the intensities of the previously treated pixels to remove the residual noise. Both adaptive and recursive methods enhanced the results, albeit at the cost of increased computing complexity. In order to enhance the performance, decision-based filters were put forth as a potential solution. Innovative approaches and tactics were used by these filters to reduce noise. A modified decision-based un-symmetric trimmed median filter [9] presented a simple detector that detected salt and pepper noise by extreme low and high intensities and then restored those identified noisy pixels by un-symmetric trimmed median of a certain sized neighbourhood. Samantaray et al. [10] used a neighborhood-based decision technique for detection, followed by a first - order neighborhood-oriented resolution for restoring noisy pixels. Neither of these filters was able to maintain the image's boundaries. Moreover, they often caused spurious noise edges and break up image edges when there was low signal-to-noise ratio. Modifications have recently been suggested to Adaptive Median Filter. Instead of using the median of the AMF, one must use an adaptive frequency median filter (AFMF) [11] to restore the grey values of distorted pixels. The frequency median helped to filter out noisy pixels while measuring the grey value of the window's centre pixel, and it emphasised the individuality of grey values. Another modification of the AMF was carried out using a filter known as Different Adaptive Modified Riesz Mean Filter (DAMRMF) [12]. DAMRMF redesigned the Adaptive Median Filter's pixel weight function and evolving criteria, improving

the filter's performance. Another current method [13] searches for outliers in a 3×3 area initially, and then looks for outliers in a larger area. Then the four neighbouring pixels are inspected for damaged pixels if the treatment pixel is disrupted. When there are outliers in the neighbourhood, the average of the four neighbours is utilized and when there are no outliers, the result of eccentrically modified trimmed mean is used to substitute the result. All three of the adaptive filters tested did a suitable job with the Salt and Pepper noise. But, the fundamental problem of these adaptive median filter techniques [11-13] is blurring, which became worsen as the adaptive windows got larger. Furthermore, some of the filter employed the median value when all values are 0 or 255, which brings with it all the downsides of a traditional median filter within these regions of the image.

There has also been recent progress made for the RVIN. A new modified median filter is proposed that can locate random value impulse noise efficiently, which is based on an improved noise classifier that has improved the total algorithm hugely [14]. Another work on the similar time frame, Zhu and Zhang [15] focused on the criteria for local brightness for restoration operation which created a new horizon in the restoration work. Localized luminosity adaptation is used to first identify visible noisy pixels, and then a difference-oriented approach is used to trace down the noisy pixels. The observable noisy pixels are restored using a weighted mean filter during the removal step. A fuzzy based morphologically oriented filter [16] has recently been developed which was very impactful. Fuzzy morphological procedures and the weighted arithmetic average aggregation function were used in the work to propose a novel filter for acoustic signals. Meanwhile, Veerakumar et al. [17] constructed an empirical mode decomposition-based noise detector with a bilateral filter for the refining and restoration of noisy pixels. In the same year, Jin and Ye [18] introduced a noise removal technique that expanded the conventional RPCA methods by manipulating the spectral domain sparseness using the rank-deficient Hankel matrix. This method was aimed at removing unwanted background noise. In impulse noise elimination studies, these two filters made a significant difference. The core issue with the empirical mode decomposition method is that it is a purely nonlinear computational operation, and the generated representation is very reliant on the specifics of the implementations. Additionally, two more filters by Veerakumar et al. [19] and Chen et al. [20] demonstrated significant gains in the impulse noise category for specialised salt and pepper noise removal. Extreme density salt and pepper noise reduction using an iterative model was made possible by Veerakumar's asymmetrically trimmed shock filter, and by Chen's detector, which employed normal distribution statistics in conjunction with native pixel intensity statistical characteristics. On the basis of sequential weightage, a neighborhood-focused median filter was used for the removal purpose. Due to the amount of iterations required, the suggested shock filter [19] requires much more time to calculate the results than the conventional techniques. Additionally, the proposed filter's higher differential equation also contributes to the increased complexity. Similarly the filter proposed by Chen et al. [20] takes higher computational time to execute due to its sequential weighting scheme. In the mean time impulse noise reduction approaches using neural networks has made an effect in the restoration field. Turkey and colleagues [21] suggested an artificial neural network (ANN) noise predictor with edge-preserving regularisation for

filtering. After that, Chen et al. suggested a blind Convolution neural network (CNN) prototype [22] employing changed training data for RVIN elimination. When employing the ANN technique [21] with the Edge preservation methodology, the filtering process is tedious and takes a very long time. Also, the blind CNN procedure [22] is computationally intensive and CNN have problems generalizing to new domains or by learning undesirable correlations rather than the targeted classes.

The theory of impreciseness becomes a burning topic recently to capture the idea of ambiguity of an uncertainty based model in any sectional area. After the invention of the fuzzy set concept [23] in 1965 portrayed by Prof. Zadeh it is widely used in numerous portions of engineering, science, and technical fields. As research goes on, people utilized these concepts in numerous application fields of mathematical modeling [24-27]. Further, the structural modifications are done by the researchers in fuzzy sections. Researchers incorporated the idea of triangular fuzzy numbers [28] and applied it to several problems [29-32] to resolve ambiguity cases. Recently, several impulse noise level works both in ordinary and digital images based on fuzzy theory like Roy et al. [33] proposed fuzzy SVM-based impulse noise detection from Gray Images; Kumar and Nagaraju [34] incorporated fuzzy entropy-based noise level detection using correlation methods for digital images; Roy et al. [35] imposed region-wise fuzzy filter approach for removal of random valued impulse noise; Kiani and Zohrevand [36] proposed fuzzy-based directional median filter method to capture the removal of fixed-value impulse noise has been established in numerous reputed journals and books. Schulte et al. [37] proposed a fuzzy impulse noise detection model; Yuksel and Besdok [38] incorporated the neuro-fuzzy noise detection model; Russo and Ramponi [39] introduced the concept of fuzzy filtering in the case of noise detection; Schulte et al. [40] manifested fuzzy filtering in case colour images; Verma and Singh [41] developed fuzzy filtering based boundary discriminative noise detection; Morillas et al. [42] introduced fuzzy-based gaussian impulse noise detection from coloured images etc.

Hence, fuzzy filters gained a lot of popularity because of their ability to deal with these uncertainties, especially in the case of impulse noise removal. Lin [43] implemented a decision-based impulse noise removal filter that used a Dempster-Shafer theory-oriented noise detection scheme and a fuzzy averaging-based noise removal methodology depending on a fixed fuzzy set. Wu and Tang [44] proposed another fuzzy filter that used rank-ordered absolute differences statistic and an extension of the non-local means concept using a fuzzy weighting scheme to remove impulse noise. Chen et al. [45] elevated the detection accuracy by designing a filter that used fuzzy estimation based on structure adaptiveness and thereby effectively restored RVIN-affected noisy pixels. The re-estimation errors of the non-noisy pixel intensities were also assessed to predict an iteration-stopping strategy. Wang et al. [46] used a detection strategy that divided the observed noisy pixels into three separate groups depending on their severity of corruption, and a removal technique to restore those noisy pixels using a weighted fuzzy switching mean filter employing distance-based criteria. Roy et al. [47] developed a novel strategy that used a support vector machine classifier to identify noise and a decision-based fuzzy filter to eliminate it.

Occasionally, in complicated operations, fuzzification and defuzzification required a significant amount of time, and it is

sometimes the case that the rules are inconsistent and do not match. However, fuzzy logic, on the other hand, is superior to other statistical approaches that rely on comprehensive human understanding of the system when dealing with ambiguous situations characterized by vague and inaccurate facts. To utilize the effectiveness of fuzzy logic, Bandyopadhyay et al. [48] employed K-means clustering methodology to identify impulsive noise coupled with a fuzzy logic-based noise reduction strategy. Both of these methods were used in recent times. The capability of these fuzzy logic-based strategies to cope with indistinctness and uncertainty contributed to their enormous effect on the field of image restoration.

According to the results of the study, researchers are focused on developing impulsive noise reduction methods based on adaptive switching, convolution neural networks, and fuzzy logic. RVIN detection is a difficult job since the pixel's alteration due to noise is random in nature, making it difficult. The researchers tried a variety of soft computing strategies [49] to help them sort out the noisy pixels, but they were unable to cope effectively with the detection process's inherent uncertainty and imprecision. The statistical filters were unable to handle these issues because of these uncertainties and ambiguous input data. Although adaptive frequency median or trimming, switching, and adaptive median filters with pixels weighting functions would improve the end results, but they cannot offer a precise answer for the restoration of impulsive noise at greater density noises. The issue of a large dependence on the details of the filter implementations affects another class of filters based on empirical mode decomposition. More advancements were made by other ANN or CNN-based techniques, but they were unable to lower the computational complexity and significant time requirements. Fuzzy logic or probability can be used as a way to handle these uncertain issues. Fuzzy logic is basically a partial dimension of truthfulness concept. Contrarily, probability deals with clear-cut statements and propositions that may either be true or untrue; where the likelihood of a proposition is the level of confidence in its veracity. As a result of the different truth degrees, fuzzy logic was finally used to resolve ambiguity and produce outcomes that were almost accurate. K-medoid Clustering was utilized in the suggested study to assemble the pixels with comparable intensities, separating the non-noisy dispersed pixels from the noisy ones. The goal of the work was to create a cluster of non-noisy pixels since their intensity fluctuation is smaller, therefore they are more likely to form a coherent group. The noisy pixels, on the other hand, are often dispersed in nature, forming small separate clusters. In addition, researchers have presented a novel fuzzy-based technique that uses fuzzy membership to choose the most influential pixel that can replace the discovered noisy pixel. In order to arrive at this conclusion, the researchers examined a variety of distance measures. Distance and SSIM (Structural Similarity Index) have been employed in our suggested study; these two factors have been combined to build a FIS (fuzzy inference system), and this has allowed us to discover which pixel is more significant. It's also feasible that certain global neighbourhood pixels might have a greater influence than some of the local neighbourhood pixels in the removal process, which hasn't been considered in different latest state-of-the-art researches. Thus, to find more precise replacements for the noisy pixels, we considered both local and global criteria in our study.

Researchers have eliminated impulse noise from the affected images in a variety of techniques, a number of which

have been already highlighted in the aforementioned literature review. To deal with the noise pattern's inherent uncertainty, various methods rely on fuzzy membership. The primary focus of the study is on the elimination of impulsive noise, which is accomplished by the use of K-medoid clustering in addition to the local and non-local non-noisy neighborhood's impacted effect on the noisy pixels guided by fuzzy measurements. A list of ingenuities is provided below in this section.

1. Leveraging K-medoid clustering for the detection of impulse noise so as to apply medoid's least average divergence to all other objects in a cluster and thus separate the noisy and non-noisy pixels in an impulse noise corrupted image.

2. It's possible that two or more clusters have the same membership value, thus the lowermost ratio of standard deviation and mean is utilized to pick a best cluster, which leads to effective noise and non-noisy pixel segregation.

3. During the noise elimination process, considering the intensities of nearby non-local non-noisy pixels that might also have an impact on the chosen noisy pixel apart from the local non-noisy pixels.

4. Constructing a Fuzzy Inference System (FIS) that takes distance and Structural Symmetry measures (SSIM) for the purpose of determining the influence value (IV) of non-local nearby pixels on the evaluated noisy pixel.

5. Utilizing fuzzy logic's ability to deal with realistic vagueness and uncertainty to find out the degree of influence of the impactful local and non-local nearest non-noisy pixels over the inspected noisy pixel and thereby execute precise noise removal operation.

Owing to the fact that 50 photographs were used to test the filter, just a few images are utilized in this situation due to the article's length restrictions. The suggested algorithms were first visually analyzed and evaluated in comparison to several state-of-the-art filters, as shown by Figures 9 and 10 in section 4 of the study. The proposed technique is then statistically evaluated using many established metrics for evaluating image quality, including the structural similarity index (SSIM), peak signal-to-noise ratio (PSNR), 'miss' and 'false' hits. Miss and false hits evaluated the K-medoid based detection's accuracy, while other metrics evaluated the final result after the whole restoration process. The proposed method yields a minimal miss and false hit value of '37841' and '9245' (out of total number of image pixels '262144' in 512×512 input image) for the intrinsic texture image "Fingerprint" at 80% noise density, as shown in Table 2 in Section 4. Additionally, the proposed KMDCIFF outperforms the previous recognized filters, producing PSNR values of 29.48 and 26.97 as well as SSIM values of 0.9288 and 0.8045 for Lena images at 80% high noise density. Finally, the windowing frame size and K-medoid method's cluster size used have been justified in the results section. Throughout all evaluation aspects, the suggested KMDCIFF was discovered to be better than all the comparable filters.

The rest of the paper is laid out as follows. For a deeper comprehension of the proposed method, the mathematical preliminaries are discussed in Section 2. Section 3 provides a step-by-step explanation of the Proposed Methodology, illustrated using flowcharts. Section 4 depicts the findings and discusses the improvements that were made in Section 3. A Section 5 on the conclusion comes at the very end of the paper.

2. MATHEMATICAL PRELIMINARIES

Definition 2.1: Interval Number: An interval number X is

denoted by $[X_L, X_R]$ and defined as $X = [X_L, X_R] = \{x: X_L \leq x \leq X_R, x \in R\}$, where R real number set and X_L and X_R generally denoted the left and right range of the interval respectively.

Lemma 2.1.1: The interval $[X_L, X_R]$ can also represented as $P(\alpha) = (X_L)^{1-\alpha}(X_R)^\alpha$ for $\alpha \in [0,1]$.

Definition 2.2: Fuzzy Set: [1] A set \tilde{S} , defined as $\tilde{S} = \{(\alpha, \mu_{\tilde{S}}(\alpha)) : \alpha \in S, \mu_{\tilde{S}}(\alpha) \in [0,1]\}$, where $\mu_{\tilde{S}}(\alpha)$ denote the membership function of \tilde{S} , is called a fuzzy set.

Definition 2.3: Triangular fuzzy number (TFN) [6]: A number $\tilde{X} = \{(a_1, a_2, a_3); \mu_{\tilde{X}}(x)\}$ will be treated as triangular fuzzy number if it satisfies the following conditions,

- (1) $\mu_{\tilde{X}}(x)$ is a continuous function in $[0,1]$
- (2) $\mu_{\tilde{X}}(x)$ is an explicitly continuously growing function in $[a_1, a_2]$
- (3) $\mu_{\tilde{X}}(x)$ will attains the value 1 at a_2
- (4) $\mu_{\tilde{X}}(x)$ is an explicitly decreasing and continuous function in $[a_2, a_3]$

Definition 2.4: Linear TFN with Symmetry: A linear TFN with symmetry normally denoted in Figure 1 as $\tilde{A}_{LS} = (s_1, s_2, s_3)$ where $s_3 - s_2 = s_2 - s_1$; whose corresponding membership function is:

$$F_{\tilde{A}_{LS}}(x) = \begin{cases} \frac{x - s_1}{s_2 - s_1} & \text{when } s_1 \leq x < s_2 \\ 1 & \text{when } x = s_2 \\ \frac{s_3 - x}{s_3 - s_2} & \text{when } s_2 < x \leq s_3 \\ 0 & \text{otherwise} \end{cases}$$

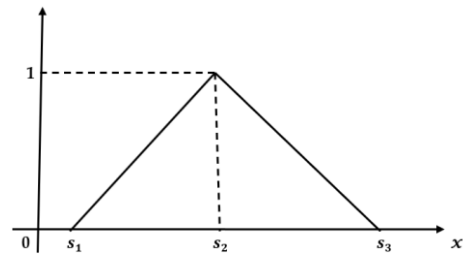


Figure 1. Linear TFN with symmetry

Definition 2.5: Linear TFN with Asymmetry: A linear TFN with asymmetry normally denoted in Figure 2 as $\tilde{A}_{LS} = (s_1, s_2, s_3)$ where $s_3 - s_2 \neq s_2 - s_1$; whose corresponding membership function is:

$$F_{\tilde{A}_{LS}}(x) = \begin{cases} \frac{x - s_1}{s_2 - s_1} & \text{when } s_1 \leq x < s_2 \\ 1 & \text{when } x = s_2 \\ \frac{s_3 - x}{s_3 - s_2} & \text{when } s_2 < x \leq s_3 \\ 0 & \text{otherwise} \end{cases}$$

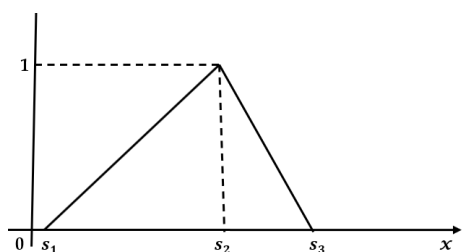


Figure 2. Linear TFN with asymmetry

Definition 2.6: Parametric form of TFN: The parametric form or Alpha (α) cut form of the TFN is:

$$F_{\tilde{A}_{LS1}}(\alpha) = s_1 + \alpha(s_2 - s_1)$$

$$F_{\tilde{A}_{LS2}}(\alpha) = s_3 - \alpha(s_3 - s_2)$$

3. PROPOSED METHODOLOGY

An impulse noise-affected grayscale image INM of dimension 512×512 is taken as an input for further processing. Given that the input noisy images in all of the standard research articles were generally 512×512 dimensions test images, it is convenient to compare the proposed findings up against the state-of-the-art filters in terms of a number of various image quality assessment metrics. Through this, the effectiveness of the proposed strategies may be swiftly assessed. Hence, 512×512 -pixel images are used as inputs as they are the accepted practice for such evaluations. Let us denote the matrix form of the image as MINM. Detection and removal are the two main components of the proposed KMDCIFF.

In this work, a detection algorithm engrossed in the K-medoid clustering technique is proposed. From the literature survey, we have identified several important factors that drove us to use the said clustering method for impulse noise detection. In general, impulse noise produces chaotic and disordered dots on the images regardless of its nature, whether fixed or random. It's tough to see any pattern in the seemingly random dots or pixel noise. In contrast, when seen as a small kernel inside a image, the noise-free pixels might form some kind of pattern or similarity. In most cases, a kernel this small represents the little portion of a larger image. So, it is more likely that the non-noisy pixel components inside a kernel are the least diverse in nature, which makes them analogous. This analogy within the non-noisy pixel elements is exploited in the way of making the proposed algorithm. The K-medoid clustering is favored because it can exploit this similarity to build clusters that can separate homogeneous non-noisy components from dispersed noisy pixels and also because of its efficacy in separating outliers.

The K-medoid clustering-based noise detection method is applied to each of the MINM matrix's 5×5 kernels, which are generated around the pixel elements. The element, located at the center (m,n) of a 5×5 kernel is denoted by C and its intensity is denoted by PV_C . Experimentation with various odd-numbered window widths was used to decide the kernel size. The 5×5 size turned out to be suitable as a result of this study. A flag image INFL, having the identical size to INM is engendered. The corresponding flag image matrix is denoted as MINFL and filled initially with '0' values. MINFL can encompass binary values (0 and 1). Let us consider a pixel (r, c) in the image INM, where $r=1, 2, 3, \dots, 512$ and $c=1, 2, 3, \dots, 512$. Once the proposed algorithm detects (r, c)th pixel as non-noisy, it sets $MINFL[r][c]$ by '0'. Although, once the (r, c)th pixel is detected as noisy, it sets $MINFL[r][c]$ by '1'. The next sub-section demonstrates the proposed detection algorithm.

3.1 Detection methodology

- i) In the primary step, the local 5×5 matrix elements are skimmed and arranged in an ascending directive. This arranged succession of elements is kept in an SRR array.
- ii) K-medoid clustering was performed on the elements of

the local 5×5 matrix's pixels, and as a result, the four clusters Cl_{S1} , Cl_{S2} , Cl_{S3} , and Cl_{S4} were formed. These clusters were formed by positioning all of the specified matrix elements in such a way that the homogeneous elements were placed in an identical cluster. The key challenge of the proposed approach is to cope with the unpredictability of the noise pattern in the images impacted by impulse noise. Since we are inspecting individual local 5×5 kernels of a contaminated image one at a time, we may imply that the non-noisy pixels of the investigated kernel are often not random in their behaviour, but the unpredictability of the noisy pixels can be inferred based on the fact that we are focusing on the randomness of the noisy pixels. Because a small kernel specifies a minuscule portion of a noisy picture, there is less chance of randomness in non-noisy pixels, but noisy pixels are typically varied in character. As a result, the chance of noisy pixels forming a cluster with a larger number of members is far lower than the probability of noisy pixels forming a cluster at all. Non-noisy pixels will, therefore, form the largest cluster, which is crucial for achieving additional noise detection goals. In the case of K-medoids clustering, rather than using the mean of the items in a cluster as a locus point as in k-means clustering, the medoid is used. A medoid is an object in the Cluster that is utmost centrally placed or has the smallest average divergence to all other objects. As a consequence, the K-medoids approach outperforms the other classic clustering algorithm in terms of noise resiliency. The non-noisy pixel intensity values observed in the largest membership cluster might be very useful in noise detection applications in the future. Experiments have shown that choosing the number of clusters to be four yields better results than choosing the number of clusters to be two, three, five, or six. Numbers bigger than six are not included since the results for clusters 5 and 6 are worsening.

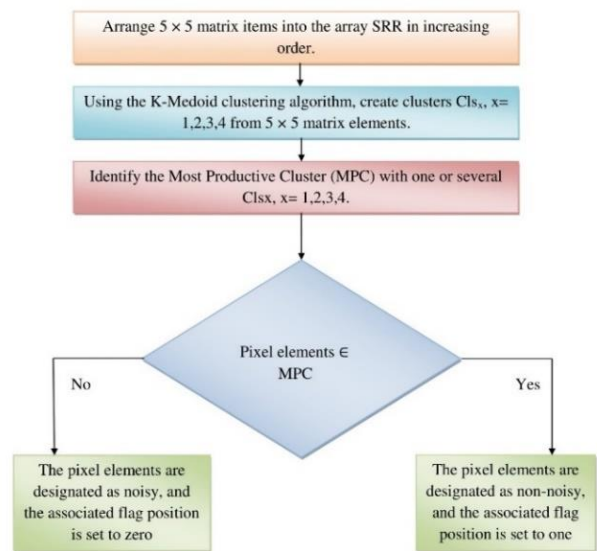


Figure 3. Flowchart of detection procedure

- iii) The Most productive cluster (MPC) is measured by comparing clusters reliant on the number of constituent elements in each cluster. MPC refers to the cluster with the greatest number of members. If more than one cluster does have maximum membership value then the ratio of standard deviation of the cluster members and the mean of the cluster members, is used to find the MPC and in this case the cluster having the lowest ratio is considered as the MPC.

iv) Finally, the pixel intensities belonging to the MPC under the MINM matrix are labeled as non-noisy ones and the rest of the pixels are detected as noisy ones by the whole detection method portrayed in Figure 3. Afterward, the detected non-noisy pixels are utilized in the subsequent noise removal procedure (Figure 4).

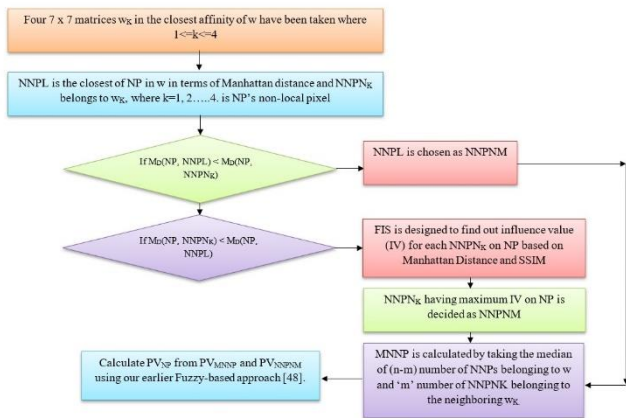


Figure 4. Flowchart of removal procedure

3.2 Removal methodology

Fuzzy logic is implemented into the suggested noise reduction strategy to take advantage of its flexibility and ability to deal with real uncertainty. The proposed fuzzy logic-based noise removal approach cleaned the damaged pixels of INM, which were identified using the proposed noise detection methodology, with high accuracy.

In order to carry out the noise reduction operation, MINFL is segmented into matrices of size 7×7 . Within each matrix, a non-noisy region denoted by the notation NP may be found at the intersection of the matrix's diagonals. Let NNPN represent a set of non-noisy pixels in a 7×7 matrix, and NPX represent the set of noisy pixels in the matrix. The suggested noise removal algorithm is executed on each of the 7×7 matrices on the whole image.

Let's consider a 7×7 matrix 'w'. Let NNPL is the closest, in terms of Manhattan Distance, the local non-noisy pixel of NP in w. Now, four 7×7 matrices in the closest affinity of 'w' have been taken. Each of these neighboring matrices of w is represented by w_k , where, $1 \leq k \leq 4$. Now the NP can be influenced by NNPL. Also, as a matter of fact, NP may get influenced by its non-local nearby non-noisy pixels belonging to w_k matrices where $k=1$ to 4. Let NNPN_k belonging to w_k , where $k=1$ to 4, is NP's, non-local non-noisy pixel, in terms of Manhattan Distance (M_D). It is to be remembered that the maximum possible Manhattan distance between NP and any non-noisy pixel in 'w' is 6. This is because NP is the center of 'w'. Let $M_D(NP, NNPL)$ is the Manhattan distance between NP and NNPL and $M_D(NP, NNPN_k)$ is the Manhattan distance between NP and NNPN_k. Now if $M_D(NP, NNPL) < M_D(NP, NNPN_k)$, then NNPL will be chosen as the most influencing non-noisy pixel denoted as NNPNM.

It is to be remembered that the maximum possible Manhattan distance between NP and any non-noisy pixel in 'w' is 6. This is because NP is the center of 'w'. Let $M_D(NP, NNPL)$ is the Manhattan distance between NP and NNPL and $M_D(NP, NNPN_k)$ is the Manhattan distance between NP and NNPN_k. Now if $M_D(NP, NNPL) < M_D(NP, NNPN_k)$, then NNPL will be chosen as the most influencing non-noisy pixel denoted as NNPNM.

If for some NNPN_k, $M_D(NP, NNPN_k) < M_D(NP, NNPL)$, then among all those NNPN_ks, the NNPN_k having the maximum influence on NP is to be found out. In order to find the most influential NNPN_k a Fuzzy Inference System (FIS) is designed. This Fuzzy Inference System (FIS) calculates an influence value (IV) for each NNPN_k on NP depending on the Manhattan distance of NP and NNPN_k and SSIM (Structural Similarity Index Measure) of 'w' and 'w_k'. Input variables, Manhattan distance, and SSIM of the FIS are defined by the following triangular membership function.

Now the fuzzy inference rules are defined as follows:

- i) If M_D is Close and SSIM is Good then IV is High.
- ii) If M_D is Close and SSIM is Average then IV is Medium.
- iii) If M_D is Close and SSIM is Bad then IV is Medium.
- iv) If M_D is Far and SSIM is Good then IV is Medium.
- v) If M_D is Far and SSIM is Average then IV is Medium.
- vi) If M_D is Far and SSIM is Bad then IV is Low.

Rule base of the proposed FIS is portrayed in Table 1.

Table 1. Rule base for proposed FIS

Variable	Category	Associated fuzzy sets' lingual elements	Triangular membership functions' intervals
Distance	Input	Close	(1, 1, 3)
		Far	(6, 6, 2)
		Good	(60, 100, 100)
SSIM	Input	Average	(40, 60, 70)
		Bad	(0, 0, 50)
		High	(65, 100, 100)
IV	Output	Medium	(45, 55, 70)
		Low	(0, 0, 40)

Figure 5 demonstrated the schematic diagram of the link between verbal phrases of triangular fuzzy number and the parameters. The triangle membership functions of two input variables are shown in Figures 6-7, and the output variable's membership function is shown in Figure 8.

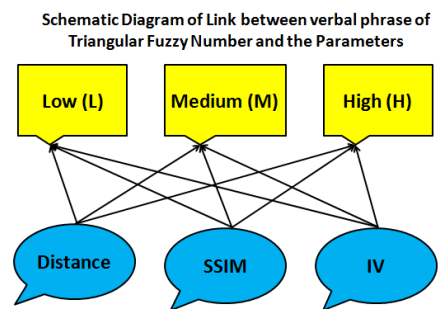


Figure 5. Schematic diagram of link between verbal phrases of triangular fuzzy number and the parameters

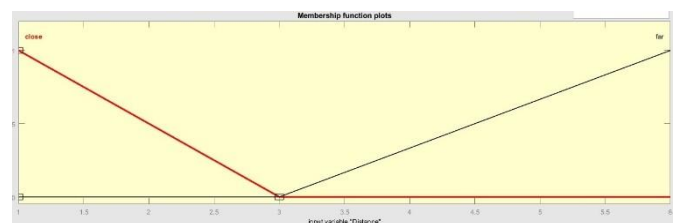


Figure 6. Triangle membership function of input variable "Distance"

Figure 6's and Figure 7's horizontal axis represents precise values of the 'Distance' and 'SSIM' input as in the range of 1 to 6 and 0 to 1 respectively. The degree of membership grades is shown by the vertical axis with the 0 to 1 range with respect to the horizontal axis values mentioned in the fuzzy sets depicted in Table 1. If an input or output variable value's degree of membership is significantly larger (closer to 1), the input or output value of the variable has a strong presence in the relevant fuzzy set.

Degrees of membership values of 1 and 0 reflect the highest degree of presence and absence of an input or output variable value in a matching fuzzy set, correspondingly. This article makes advantage of the triangular membership function's characteristic, which is distinguished by its mathematical precision. It has three arguments, a_1 , a_2 , and a_3 , in which the membership function $\mu_{\bar{x}}(x)$ is defined for every value x in Definition 2.3 and 2.4 of Chapter 2. These arguments were discovered via the authors' research on the suggested system. As was already indicated, "Distance" and "SSIM" are the two input variables used. The lingual members of the corresponding fuzzy sets for the distance variable are "Close" and "Far", respectively. The linguistic members of the linked fuzzy sets for the SSIM variable are, in order, "Good," "Average," and "Bad". At the end, "High," "Medium," and "Low" are the linguistic constituents of the linked fuzzy sets representing the IV output variable. The IV of $NNPN_K$ on NP is now determined for every $NNPN_K$ where $M_D(NP, NNPN_K) < M_D(NP, NNPL)$ and $NNPN_K$ having maximum IV on NP is decided as the most influencing non-noisy pixel (NNPNM) neighboring to NP and its pixel intensity is denoted as PV_{NNPNM} . Now, NNPL is already obtained, and apart from it; MNNP (median pixel of the non-noisy pixels of the window) can also have an influence on NP. So, in that case, there may exist some non-noisy pixels that are not NNPL but belong to the window 'w'. Let's denote those pixels as NNPNK (non-noisy pixel not close) where $NNPNK \in w$. Again, it may be possible for some NNPNKs: $M_D(NP, NNPNK) > M_D(NP, NNPN_K)$. So, the above situation implies that the $NNPN_K$ are closer to NP rather than the NNPNK. In these circumstances, those NNPNKs are excluded from the calculation of MNNP and, instead, the NNPNKs that are closer to NP are included. Say, there are 'n' no of non-noisy pixels in 'w'. Now, it has to be found out that, how many of these non-noisy pixels have $M_D(NP, NNPNK) > M_D(NP, NNPN_K)$.

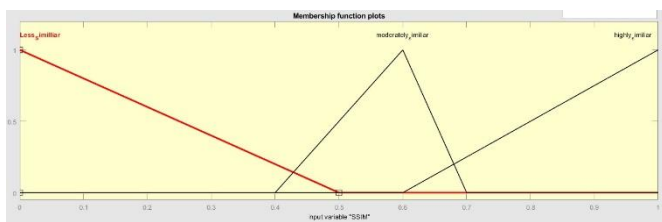


Figure 7. Triangle membership function of input variable "SSIM"

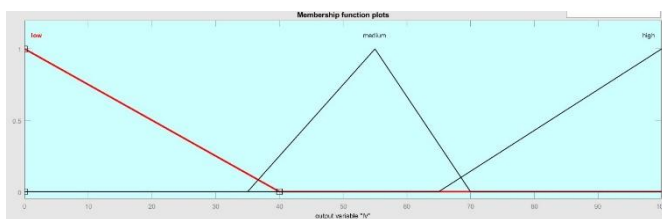


Figure 8. Triangle membership function output variable "IV"

Let the number of such NNPNKs be 'm'. Then, $(n-m)$ number of non-noisy pixels (NNP) in 'w' having $M_D(NP, NNP) < M_D(NP, NNPN_K)$ are considered in the calculation of MNNP, and the rest of the 'm' number of pixels will be those NNPNKs that are having $M_D(NP, NNPN_K) < M_D(NP, NNPNK)$.

Thus, MNNP is calculated by taking the median of $(n-m)$ number of NNPs belonging to w and 'm' number of NNPNK belonging to the neighboring w_K . Its pixel intensity value is denoted as PV_{MNNP} . Then PV_{NP} is calculated by utilizing PV_{MNNP} and PV_{NNPNM} using self-published earlier fuzzy oriented approach [48]. The median pixel PV_{MNNP} of the noisy pixel's non-noisy neighbours and the noisy pixel's closest non-noisy neighbour PV_{NNPNM} are used as reference pixels. It is anticipated that the noisy pixel's estimated pixel intensity value would fall somewhere in the middle of the two reference pixel intensities. To get the predicted pixel intensity value, it is crucial to know how much impact the aforesaid two reference pixels have on the noisy pixel. Using the term "induction factor", we may describe how much an external reference pixel affects an internal noisy pixel. For each of the reference pixels, there is an induction factor on the noisy pixel, and we need to determine which one has the greater induction factor. However, we cannot completely disregard the other reference pixel's induction factor. Fuzzy logic is utilized to deal with ambiguity and uncertainty, and it has successfully enlightened us by accurately computing the induction factors of two reference pixels on the noisy pixel. This is made possible by fuzzy logic's capacity to deal realistically with ambiguity and uncertainty.

A fuzzy set called "Near" is created using a fuzzy membership function called "Near". Near takes as an input the Manhattan distance between the coordinate position of the noisy pixel in the corrupted picture and the coordinate position of a reference pixel in the damaged image. As an output, "Near" produces the membership value of that Manhattan distance in the fuzzy set "Near". Manhattan distance membership value between noisy pixels and "Near" reference pixels reflect the influence of that reference pixel on the noisy one. The induction factor ranges from 0 to 1. Zero represents no induction, while one indicates maximum induction. Reference pixels that have an induction factor of 1 are given preference over other reference pixels that do not have induction factors of 1, and this preference is used to determine which of the two reference pixels should be used to calculate the predicted pixel intensity value of the noisy pixel.

The mean of the two reference pixel intensity values is allocated as the predicted pixel intensity value if both the reference pixels have the same induction factors on the noisy pixel. This is referred to as a "neutral" scenario. If the induction factor of the reference pixel is greater than that of another reference pixel then the situation is referred as non-neutral or biased scenario. In biased scenario, the predicted pixel intensity value of the noisy pixel varies from its neutral scenario value and tends to approach the pixel intensity value associated with the reference pixel having greater induction factor on the noisy pixel. The deviation is derived by multiplying the 1/2 of the absolute difference between the intensity values of two reference pixels with the absolute difference between the induction factors of two reference pixels on the noisy pixel. Predicted pixel intensity value PV_{NP} of the noisy pixel is calculated by associating the deviation to the neutral scenario value.

4. RESULTS AND DISCUSSION

This section investigates the qualitative and quantitative comparative findings for FVIN and RVIN. A comparison of the proposed KMDCIFF with eight existing techniques is made for both RVIN and FVIN. An Intel Core i5 CPU and 8GB of RAM having MATLAB 2018a was used for all of the testing, which took place on several different test images featuring varying noise levels. The performance of the proposed filter is evaluated and objectively compared with the help of measurements of the peak signal-to-noise ratio (PSNR), as well as the structural similarity index (SSIM).

The following is the interpretation of PSNR, expressed in decibels (dB):

$$PSNR = 10 \log_{10} \frac{255^2}{MSE} \quad (1)$$

$$MSE = \left(\sum_{K,L} \frac{(Org(k,l) - Dn(k,l))^2}{K \times L} \right) \quad (2)$$

where, Org=Original Image, Dn=De-noised image, K=No. of rows and L=No. of Columns.

It is appropriate to observe the original and restored images using SSIM. According to the SSIM definition,

$$SSIM(i,j) = \frac{(2\psi_i\psi_j + \xi_1)(2\beta_{ij} + \xi_2)}{(\psi_i^2 + \psi_j^2 + \xi_1)(\beta_i^2 + \beta_j^2 + \xi_2)} \quad (3)$$

where, image i and Image j each have a mean value of ψ_i and, ψ_j respectively. Image i 's standard deviation is shown by β_i and image j 's standard deviation is shown by β_j and the constants are ξ_1 and ξ_2 . β_{ij} is the co-variance between i and j .

Lena and Baboon, two well-known test photos, exhibit the visual output of the suggested filter. Even though 50 images were used to test the filter, only the two shown above are used in this circumstance owing to length constraints on the article. Figure 9 provides an interpretation of the visual output comparison of the proposed filter in contrast to the recent filters at a variety of noise levels that are influenced by FVIN for Baboon image. In addition, Figure 10 shows how the suggested filter's output varies with the applied input when affected by RVIN for a standard Lena image. As can be observed in both Figure 9 and Figure 10, the recommended filter has produced visually noticeable improvements for impulse noise pattern. These improvements can be seen in both Figure 9 and Figure 10.

Typically, the detecting method has a major influence on the following restoration process. This algorithm's detection approach is examined for both the RVIN and FVIN, although the assessment of the detector's performance will be mostly focussed on its results for RVIN, because RVIN is substantially more difficult to identify than FVIN. The suggested algorithm's detection accuracy is evaluated using "miss" and "false-hit" metrics for 512×512 test images. The term "miss" refers to the number of legitimately corrupted pixels that the proposed detector incorrectly identifies as non-corrupted, while the term "false-hit" refers to the number of legitimately non-corrupted pixels that the suggested detector incorrectly identifies as corrupted. A "false-hit" number, rather than a "miss" value, is a far more significant aspect from a logical standpoint. A high false-hit value may lead to the

inaccurate identification of a genuine non-corrupted pixel and hence have a significant impact on the eradication process.

Experimental images with varying noise levels are included in Table 2 to illustrate the proposed detector's 'miss' and 'false-hit' scores, respectively. The Lena, Goldhill, and Baboon images show minimum miss and false hit scores with the proposed KMDCIFF. The technique has also been checked on more complex images as Bridge, Boat, Barbara, where it performed well, although with relatively less accuracy. The fingerprint picture yielded average results since it consists of textural qualities and fine minutiae. On the other hand, when the aggregate noise from each of the test images is factored in, the recommended strategy produces extremely compelling outcomes.

Table 2. Detection result of the proposed KMDCIFF by miss and false-hit for different images

Noise	Images	60%ND		80%ND	
		miss	false-hit	miss	false-hit
RVIN	Lena	16870	5069	29874	7617
	Goldhill	17254	5354	30198	7868
	Baboon	19874	5984	32568	8245
	Boat	18471	5520	31101	7996
	Barbara	21548	6120	35481	8756
	Cameraman	17056	5111	30150	7715
	Fingerprint	25487	7005	37841	9245
FVIN	Lena	15478	4580	27659	6548
	Goldhill	16351	4759	28655	6785
	Baboon	18459	5689	29593	7246
	Boat	17005	5115	30254	6943
	Barbara	19985	5945	31848	7545
	Cameraman	15984	4695	28159	6677
	Fingerprint	22167	6519	34597	8563

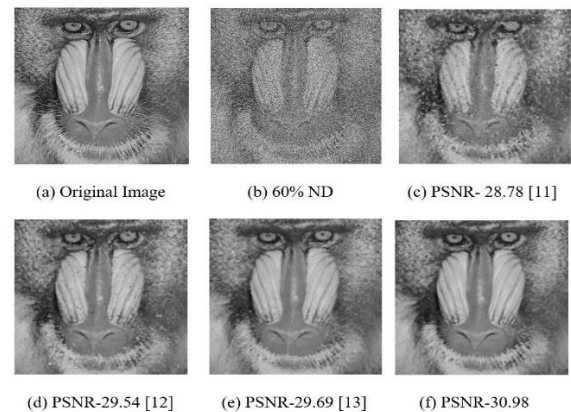


Figure 9. Comparison of proposed work with other recent filters for FVIN

Table 3 and Table 4 compared the proposed filter's performance based on PSNR and SSIM up against the state-of-the-art filters for RVIN and FVIN on standard test images, such as: Lena, Barbara, and Baboon. The two forms of noise that were discussed earlier each cause images to have either fixed or random spots, which results in an exaggerated appearance. The proposed KMDCIFF handled both noise models effectively even at high noise densities which is noticeable in Table 3. The proposed KMDCIFF produces exceptional PSNR of 29.48 dB, 25.36 dB, 26.22 db and 26.97dB, 23.98 dB, 24.01 dB for Lena, Barbara, and Baboon images at 80% noise density for FVIN and RVIN respectively.

Table 3. Restoration results in terms of PSNR

Image	Noise	Filters	Noise Density		
			40%	60%	80%
Lena	FVIN	SVMF [47]	31.24	27.71	24.86
		AFSWMF [46]	31.23	27.03	24.46
		EMDABF [19]	36.00	31.25	27.01
		VEERA [17]	34.20	31.05	27.38
		ASWM [20]	34.74	32.82	27.93
		AFMF [11]	33.71	30.46	28.46
		DAMRmF [12]	35.55	32.72	29.37
		DBNATMTF [13]	29.58	27.69	25.95
		KMDCIFF	35.45	32.75	29.48
		ANN [21]	30.32	27.22	23.65
	RVIN	SAFE [45]	32.18	28.38	24.46
		EMDABF [19]	35.26	30.55	26.35
		JIN [18]	30.62	28.68	24.65
		CHEN [22]	31.17	28.29	24.36
		DBMF [14]	13.52	12.75	11.65
		ZHU [15]	27.19	25.02	23.25
		AWAM [16]	33.91	29.67	25.12
		KMDCIFF	34.68	32.02	26.97
		SVMF [47]	26.61	22.93	19.95
		AFSWMF [46]	29.73	25.01	22.19
Barbara	FVIN	EMDABF [19]	30.20	27.07	23.78
		VEERA [17]	31.10	27.03	23.93
		ASWM [20]	31.31	27.32	24.11
		AFMF [11]	29.62	26.98	24.56
		DAMRmF [12]	30.19	27.06	25.21
		DBNATMTF [13]	29.58	26.88	24.86
		KMDCIFF	30.78	27.68	25.36
		ANN [21]	27.66	24.34	21.11
		SAFE [45]	27.97	25.08	21.05
		EMDABF [19]	25.98	22.55	19.87
	RVIN	JIN [18]	28.69	26.12	23.56
		CHEN [22]	30.98	25.87	22.13
		DBMF [14]	11.05	10.65	10.22
		ZHU [15]	26.25	24.26	22.35
		AWAM [16]	30.02	26.12	23.09
		KMDCIFF	30.28	26.51	23.98
		SVMF [47]	26.01	22.12	18.72
		AFSWMF [46]	29.17	24.55	21.48
		EMDABF [19]	30.85	27.98	24.56
		VEERA [17]	30.96	26.78	23.23
Baboon	FVIN	ASWM [20]	33.34	30.92	26.13
		AFMF [11]	31.25	28.78	25.48
		DAMRmF [12]	31.94	29.54	26.02
		DBNATMTF [13]	32.05	29.69	26.12
		KMDCIFF	32.21	30.98	26.22
		ANN [21]	27.14	23.88	20.17
		SAFE [45]	27.67	24.72	20.65
		EMDABF [19]	25.87	22.15	19.24
		JIN [18]	22.48	19.25	16.59
		CHEN [22]	32.25	27.48	23.47
	RVIN	DBMF [14]	13.12	12.02	10.96
		ZHU [15]	30.74	26.14	22.59
		AWAM [16]	31.25	27.06	23.56
		KMDCIFF	31.88	27.57	24.01

a noise density of 40% and a similarity of over 66% at an extreme noise density of 80%.

Table 4. Restoration results in terms of SSIM

Image	Noise	Filters	Noise Density		
			40%	60%	80%
Lena	FVIN	SVMFF [47]	0.9134	0.8347	0.8132
		AFSWMF [46]	0.9305	0.8349	0.8176
		EMDABF [19]	0.9445	0.8525	0.8245
		VEERA [17]	0.9441	0.8698	0.8269
		ASWM [20]	0.9874	0.9702	0.9212
		AFMF [11]	0.9749	0.9624	0.9215
		DAMRmF [12]	0.9854	0.9701	0.9198
		DBNATMTF [13]	0.9548	0.9343	0.8909
		KMDCIFF	0.9862	0.9748	0.9288
		ANN [21]	0.8747	0.7987	0.7125
	RVIN	SAFE [45]	0.9199	0.8461	0.7573
		EMDABF [19]	0.9199	0.8194	0.7539
		JIN [18]	0.9268	0.8295	0.7749
		CHEN [22]	0.8916	0.7931	0.7321
		DBMF [14]	0.8342	0.7724	0.7002
		ZHU [15]	0.8648	0.7995	0.7254
		AWAM [16]	0.9146	0.8254	0.7712
		KMDCIFF	0.9178	0.8621	0.8045
		SVMF [47]	0.8614	0.7865	0.7123
		AFSWMF [46]	0.9047	0.8258	0.6903
Barbara	FVIN	EMDABF [19]	0.9099	0.8318	0.6927
		VEERA [17]	0.9089	0.8343	0.7113
		ASWM [20]	0.9798	0.9479	0.8254
		AFMF [11]	0.9645	0.9358	0.8142
		DAMRmF [12]	0.9541	0.9124	0.7548
		SVMF [47]	0.9245	0.8752	0.7124
		KMDCIFF	0.9771	0.9512	0.8355
		ANN [21]	0.7458	0.7125	0.6125
		SAFE [45]	0.8668	0.7362	0.6425
		EMDABF [19]	0.7698	0.7249	0.6358
	RVIN	JIN [18]	0.7795	0.7459	0.6597
		CHEN [22]	0.7549	0.7198	0.6216
		DBMF [14]	0.7124	0.6584	0.5987
		ZHU [15]	0.7654	0.7259	0.6458
		AWAM [16]	0.7785	0.7452	0.6874
		KMDCIFF	0.8459	0.7698	0.6987
		SVMF [47]	0.8543	0.7737	0.6772
		AFSWMF [46]	0.8816	0.8149	0.6826
		EMDABF [19]	0.8963	0.8198	0.6785
		VEERA [17]	0.8951	0.8214	0.6958
Baboon	FVIN	ASWM [20]	0.9788	0.9451	0.8245
		AFMF [11]	0.9674	0.9247	0.7961
		DAMRmF [12]	0.9586	0.9324	0.8009
		SVMF [47]	0.9524	0.9148	0.8124
		KMDCIFF	0.9745	0.9462	0.8452
		ANN [21]	0.7267	0.6859	0.5579
		SAFE [45]	0.7585	0.6987	0.6077
		EMDABF [19]	0.7412	0.6805	0.5989
		JIN [18]	0.7698	0.7015	0.6125
		CHEN [22]	0.7349	0.6789	0.5896
	RVIN	DBMF [14]	0.7005	0.6124	0.5486
		ZHU [15]	0.7537	0.7104	0.6245
		AWAM [16]	0.7658	0.7195	0.6477
		KMDCIFF	0.8048	0.7259	0.6654

Furthermore, the proposed KMDCIFF yielded SSIM of 0.9288, 0.8355, 0.8452 and 0.8045, 0.6987, 0.6654 for Lena, Barbara, and Baboon images at 80% noise density for FVIN and RVIN respectively. It is pertinent from both Table 3 and Table 4 that, KMDCIFF outperformed current credible filters at a variety of noise levels, particularly at larger noise densities. According to the analysis, the proposed filter accomplishes 80% similarity for all images at a high noise density of 80% with reference to FVIN and also over 97% resemblance at a moderate noise density of 40%. For RVIN, the recommended KMDCIFF have a similarity of over 80% at

These results justify that the proposed technique is capable of restoring the structure of the images to an excellent level post restoration.

The proposed experimentation had been carried out between three to four times for each of the reference images and noise densities, and this had been done for both FVIN and RVIN. It was discovered that the divergence of the PSNR and

SSIM values collected were between the ranges of 0.06-0.18 DB and 0.045-0.183 respectively, both of which are considered to be extremely trivial. Consequently, it became evident that the variation in the findings was within a tolerable range.

The performance of the proposed KMDCIFF, measured in terms of PSNR and SSIM, is shown for a range of images in Tables 5 and 6. From a total of 50 images tested, the following exhibits the outcomes of random 4 images after implementing the filter proposed. Table 5 demonstrates that the proposed filter generates an outstanding PSNR of 23.05 db and SSIM of 0.6954 for an intricate fingerprint image that has been damaged by RVIN at a high noise level of 80%. In addition, at a mid-level noise of 40%, the proposed filter delivers notable PSNR and SSIM performances, that is visible from the Table 5 and 6 respectively. Table 6 demonstrates the proposed filter's performance for FVIN. The KMDCIFF yields a PSNR of 24.68 db and an SSIM of 0.7525 for the same Fingerprint image at a significant noise density of 80%, and it also performs healthy at mid-level and low-level noise densities. In order to determine the appropriate window size for the suggested technique, an approach based on trial and error was used. Following the successful application of the method across a variety of odd-numbered window sizes, it was determined that the 5×5 and 7×7 grid sizes were suitable for the proposed detection and correction strategy.

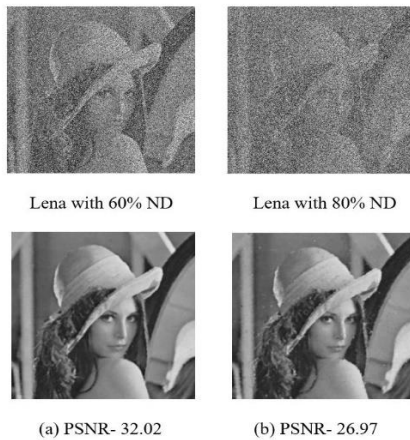


Figure 10. Visual demonstration of the proposed filter's performance for RVIN at various noise densities

Table 5. Restoration outcomes of proposed KMDCIFF for diverse images distorted by RVIN

Approach	Goldhill	Boat	Cameraman	Fingerprint	
PSNR	40%	33.98	33.71	34.35	29.67
	60%	31.72	31.47	31.91	26.21
	80%	26.01	25.67	26.32	23.05
SSIM	40%	0.9019	0.8997	0.9115	0.8547
	60%	0.8506	0.8467	0.8594	0.7854
	80%	0.7844	0.7757	0.7988	0.6954

Table 6. Restoration outcomes of proposed KMDCIFF for diverse images distorted by FVIN

Approach	Goldhill	Boat	Cameraman	Fingerprint	
PSNR	40%	34.17	34.11	35.02	31.12
	60%	32.01	31.88	32.24	28.76
	80%	26.82	25.99	27.38	24.68
SSIM	40%	0.9725	0.9658	0.9802	0.8994
	60%	0.9459	0.9241	0.9654	0.8125
	80%	0.9188	0.8897	0.9047	0.7525

It is clear from Table 7 that the proposed technique generated the best PSNR values, when both of the nominated odd-numbered window sizes were picked.

Table 7. Performance measure of the proposed KMDCIFF based on window wise for Lena image

Noise	Window Size		Noise Densities			
	Detection	Removal	40%	60%	80%	
RVIN	3×3	3×3	31.98	30.48	24.49	
		5×5	32.54	31.12	25.23	
		7×7	32.66	31.16	25.34	
	5×5	3×3	32.74	31.24	25.45	
		5×5	33.17	31.69	26.08	
		7×7	34.68	32.02	26.97	
		3×3	32.98	31.54	25.98	
		7×7	5×5	34.22	31.78	26.12
			7×7	34.48	31.94	26.77
			3×3	34.12	31.21	25.19
FVIN	3×3	5×5	34.48	31.78	26.15	
		7×7	35.04	32.08	27.09	
		3×3	34.98	32.01	26.94	
	5×5	5×5	35.11	32.27	27.25	
		7×7	35.45	32.75	28.01	
		3×3	35.06	32.07	27.11	
		7×7	5×5	35.14	32.24	27.21
			7×7	35.24	32.47	27.58

Prior to execution of a removal method, detection is the most important function of a filter. Cluster size must be specified in order for the suggested approach to use K-medoid clustering to differentiate noisy from non-noisy components in detection. Because the detection method uses a window size of 5×5 , as was mentioned before, the 25 elements of that window will be divided into their own distinct clusters when the K-medoid algorithm is used. Choosing a large number of clusters may undercut clustering's goal by generating many little clusters, most of which will have scattered noisy pixel values. As a result, it will be difficult to find a cluster with the most non-noisy members. Consequently, a smaller cluster size was chosen, and the research was carried out through trial and error. Table 8 shows that, when tested on a variety of images, a cluster size of '4' produced the maximal performance for the recommended technique.

Table 8. Performance measure of the proposed KMDCIFF based on cluster size for Lena image

Noise	Images	Cluster Size		
		3	4	5
FVIN	Lena	32.54	32.75	32.05
	Goldhill	31.88	32.01	31.65
	Baboon	30.14	30.98	29.92
	Barbara	27.09	27.68	26.87
	Cameraman	31.94	32.24	31.54
	Boat	31.45	31.88	30.99
	Fingerprint	27.98	28.76	26.89
	Lena	31.55	32.02	31.05
	Goldhill	31.21	31.71	30.95
	Baboon	26.88	27.58	25.75
RVIN	Barbara	25.45	26.51	24.97
	Cameraman	31.29	31.91	30.74
	Boat	30.73	31.47	30.01
	Fingerprint	25.06	26.21	23.82

To summarize, KMDCIFF outperforms other modern filters in several aesthetic and quantitative aspects.

4.1 Discussion

The aforementioned results, whether qualitative or quantitative, emphasize and validate the significance of the whole study. K-medoid clustering's detection ability was strengthened mostly by the 'miss' and 'false' hits, which served as the proposed work's foundation. The succeeding procedure may have been severely impeded if an actual non-corrupted pixel is incorrectly identified due to a greater false-hit value. Table 1 shows that with the proposed method, the false-hit numbers are much reduced, demonstrating that the work's strength factor may undoubtedly aid in achieving better removal outcomes. Secondly, the proposed algorithm performed significantly better than those of the state-of-the-art approaches, as shown in Tables 3 and 4 with respect to major two metrics (PSNR and SSIM). In addition, Manhattan Distance and SSIM were used in the development of a Fuzzy Inference System that produced an 'IV' that determined the effect of local as well as nearby adjoining windows' non-noisy pixels on the inspected noisy pixel. As seen in Table 1, "miss" and "false-hits" had an enormous influence on the detection results. To get the best results, the algorithm is run three times for each different noise density, and only very little variations in the results are seen, defining the method's stability. In furthermore, the proposed work has been tested on a variety of images with varying levels of noise, some of which are displayed in Tables 5 and 6. It is clear that the suggested strategy performed well on diverse images that were completely unrelated to each other. Furthermore, the choice of cluster size and window size during the K-medoid clustering phase and the whole operation is critical since the noise might be random in nature. In Table 8, a variety of cluster modifications and their impact on the final result have been shown, and as a result, the ideal size of the cluster has been selected. In a similar fashion, the differences in window size and the results of those variations have been depicted in Table 7, and the best combination being found. Rigorous testing has been performed on a number of different combinations in order to identify the one that is acceptable for picking both the cluster size and the window sizes.

4.2 Advantages of work

In comparison to other partitioning methods, the K-medoid Algorithm is quick, capable of approximating in a defined sequence of steps, and is significantly less prone to outliers. Additionally, Fuzzy logic is a natural option to handle the random aspect of impulse noises since it is designed to deal with ambiguous and uncertain circumstances. Moreover, the proposed method also considered influential non-local non-noisy pixels as an option during the fuzzy implementation for the impulse noise reduction strategy, in addition to the local non-noisy pixels. When taken as a whole, the quantitative and qualitative findings show that the suggested method outperforms the state-of-the-art filters.

4.3 Limitations of work

The first k medoids are selected at random, thus subsequent iterations using the same data may yield different outcomes but the deviation is negligible. The succeeding rounds of K-medoid based detection combined with the fuzzy inference system to produce the final result is a precise but time-consuming process. Overall, the suggested strategy produces

better results across the board but at the expense of time.

5. CONCLUSIONS

This work presented a seamless combination of K-medoid clustering-based noise detection with fuzzy logic-based noise reduction. During the detection phase, K-medoid clustering is used for establishing cluster identification to select the most effective cluster that divided non-noisy and noisy pixels. After that, a mix of local and global fuzzy criteria was used to replace the noisy pixels in the removal technique. K-medoid's use in the detection process boosted the suggested strategy in its first stages. The ability of its rigorous similarity-oriented grouping to differentiate exactly between noisy and non-noisy pixels boosted the recommended technique and minimized the propensity toward blurring. Additionally, the significance of non-local non-noisy pixels' influence on noise removal established a standard that opened up new possibilities for the area of image restoration. On the basis of detection accuracy by K-medoid clustering and fuzzy logic's intrinsic capacity to create near correct results from the uncertain dataset, together with the use of non-local neighboring non-noisy global pixels influence in the filtering scheme, the proposed filter is distinct from and more effective than the state-of-the-art filters. The effectiveness of the method is evaluated on a variety of images in terms of the PSNR and SSIM metrics. Additionally, the window size and cluster size selection processes have been analyzed and validated for their respective effectiveness. The suggested KMDCIFF has been found improved to the other recent filters in a number of ways. In future, more accurate results may be achieved with new optimized procedures by developing new technology that raises the PSNR value of the restored image. In addition, we would want to do in-depth research minute edge detection principles and on the many other categories of noise patterns. The article has no conflicts of interest for the authors.

ACKNOWLEDGMENT

This work is supported by and carried out at the Center for Machine Learning and Excellence, SKFGI and is dedicated to Ms. Sonali Banerjee for her relentless inspiration.

REFERENCES

- [1] Thakur, R.S., Chatterjee, S., Yadav, R.N., Gupta, L. (2021). Image de-noising with machine learning: A review. IEEE Access. <https://doi.org/10.1109/ACCESS.2021.3092425>
- [2] Bandyopadhyay, A., Deb, K., Das, A., Bag, R. (2020). Manhattan distance based nearest vicinity guided filter design for high density salt and pepper noise removal. In 2020 IEEE 1st International Conference for Convergence in Engineering (ICCE), pp. 184-188. <https://doi.org/10.1109/ICCE50343.2020.9290739>
- [3] Reddy, C.K., Krishna, Y.S., Sai, M.L., Rahul, T.R., Ram, N.S., Singh, A. (2022). A review of image denoising using machine learning. *Futuristic Sustainable Energy and Technology*, 281-290.
- [4] Bandyopadhyay, A., Deb, K., Das, A., Bag, R. (2021). Random valued impulse noise detection using fuzzy c-

- means clustering technique. In: Satapathy, S.C., Bhateja, V., Favorskaya, M.N., Adilakshmi, T. (eds) *Smart Computing Techniques and Applications. Smart Innovation, Systems and Technologies*. https://doi.org/10.1007/978-981-16-0878-0_39
- [5] Nair, M.S., Mol, P.A. (2013). Direction based adaptive weighted switching median filter for removing high density impulse noise. *Computers & Electrical Engineering*, 39(2): 663-689. <https://doi.org/10.1016/j.compeleceng.2012.06.004>
- [6] Yuan, C., Li, Y. (2015). Switching median and morphological filter for impulse noise removal from digital images. *Optik*, 126(18): 1598-1601. <https://doi.org/10.1016/j.ijleo.2015.05.032>
- [7] Meher, S.K., Singhawat, B. (2014). An improved recursive and adaptive median filter for high density impulse noise. *AEU-International Journal of Electronics and Communications*, 68(12): 1173-1179. <https://doi.org/10.1016/j.aeue.2014.06.006>
- [8] Lee, J.Y., Jung, S.Y., Kim, P.W. (2018). Adaptive switching filter for impulse noise removal in digital content. *Soft Computing*, 22(5): 1445-1455. Chen, W. K. (1993). *Linear Networks and Systems*. Wadsworth, Belmont, 123-135. <https://doi.org/10.1007/s00500-017-2843-9>
- [9] Esakkirajan, S., Veerakumar, T., Subramanyam, A.N., PremChand, C.H. (2011). Removal of high density salt and pepper noise through modified decision based unsymmetric trimmed median filter. *IEEE Signal Processing Letters*, 18(5): 287-290. <https://doi.org/10.1109/LSP.2011.2122333>
- [10] Samantaray, A.K., Kanungo, P., Mohanty, B. (2018). Neighbourhood decision based impulse noise filter. *IET Image Processing*, 12(7): 1222-1227. <https://doi.org/10.1049/iet-ipr.2017.1372>
- [11] Erkan, U., Enginoğlu, S., Thanh, D.N. (2020). Adaptive frequency median filter for the salt and pepper denoising problem. *IET Image Processing*, 14(7): 1291-1302. <https://doi.org/10.1049/iet-ipr.2019.0398>
- [12] Memiş, S., Erkan, U. (2021). Different adaptive modified riesz mean filter for high-density salt-and-pepper noise removal in grayscale images. *Avrupa Bilimve Teknoloji Dergisi*, (23): 359-367. <https://doi.org/10.31590/ejosat.873312>
- [13] Vasanth, K. (2021). A decision based neighbourhood referred asymmetrically trimmed modified trimean for the removal of high density salt and pepper noise in images and videos. *Wireless Personal Communications*, 120(4): 2585-2609. <https://doi.org/10.1007/s11277-021-08547-4>
- [14] Ma, C., Lv, X., Ao, J. (2019). Difference based median filter for removal of random value impulse noise in images. *Multimedia tools and applications*, 78(1): 1131-1148. <https://doi.org/10.1007/s11042-018-6442-2>
- [15] Zhu, Z., Zhang, X. (2022). A random-valued impulse noise removal algorithm via just noticeable difference threshold detector and weighted variation method. *International Journal of Computers and Applications*, 44(2): 187-200. <https://doi.org/10.1080/1206212X.2020.1719309>
- [16] González-Hidalgo, M., Massanet, S., Mir, A., Ruiz-Aguilera, D. (2021). Impulsive noise removal with an adaptive weighted arithmetic mean operator for any noise density. *Applied Sciences*, 11(2): 560. <https://doi.org/10.3390/app11020560>
- [17] Veerakumar, T., Subudhi, B.N., Esakkirajan, S. (2019). Empirical mode decomposition and adaptive bilateral filter approach for impulse noise removal. *Expert Systems with Applications*, 121: 18-27. <https://doi.org/10.1016/j.eswa.2018.12.009>
- [18] Jin, K.H., Ye, J.C. (2017). Sparse and low-rank decomposition of a Hankel structured matrix for impulse noise removal. *IEEE Transactions on Image Processing*, 27(3): 1448-1461. <https://doi.org/10.1109/TIP.2017.2771471>
- [19] Veerakumar, T., Subudhi, B.N., Esakkirajan, S., Pradhan, P.K. (2019). Iterative adaptive unsymmetric trimmed shock filter for high-density salt-and-pepper noise removal. *Circuits, Systems, and Signal Processing*, 38(6): 2630-2652. <https://doi.org/10.1007/s00034-018-0984-4>
- [20] Chen, J., Zhan, Y., Cao, H. (2019). Adaptive sequentially weighted median filter for image highly corrupted by impulse noise. *IEEE Access*, 7: 158545-158556. <https://doi.org/10.1109/ACCESS.2019.2950348>
- [21] Turkmen, I. (2016). The ANN based detector to remove random-valued impulse noise in images. *Journal of Visual Communication and Image Representation*, 34: 28-36. <https://doi.org/10.1016/j.jvcir.2015.10.011>
- [22] Chen, J., Zhang, G., Xu, S., Yu, H. (2019). A blind CNN denoising model for random-valued impulse noise. *IEEE Access*, 7: 124647-124661. <https://doi.org/10.1109/ACCESS.2019.2938799>
- [23] Zadeh, L.A. (1965). Fuzzy sets. *Information and Control*, 8(5): 338-353. [https://doi.org/10.1016/S0019-9958\(65\)90241-X](https://doi.org/10.1016/S0019-9958(65)90241-X)
- [24] Maiers, J., Sherif, Y.S. (1985). Applications of fuzzy set theory. *IEEE Transactions on Systems, Man, and Cybernetics*, (1): 175-189. <https://doi.org/10.1109/TSMC.1985.6313408>
- [25] Chakraborty, A., Mondal, S.P., Alam, S., Ahmadian, A., Senu, N., De, D., Salahshour, S. (2019). The pentagonal fuzzy number: Its different representations, properties, ranking, defuzzification and application in game problems. *Symmetry*, 11(2): 248. <https://doi.org/10.3390/sym11020248>
- [26] Chakraborty, A., Maity, S., Jain, S., Mondal, S.P., Alam, S. (2021). Hexagonal fuzzy number and its distinctive representation, ranking, defuzzification technique and application in production inventory management problem. *Granular Computing*, 6(3): 507-521. <https://doi.org/10.1007/s41066-020-00212-8>
- [27] Maity, S., Chakraborty, A., De, S.K., Mondal, S.P., Alam, S. (2020). A comprehensive study of a backlogging EOQ model with nonlinear heptagonal dense fuzzy environment. *RAIRO-Operations Research*, 54(1): 267-286. <https://doi.org/10.1051/ro/2018114>
- [28] Anand, M.C.J., Bharatraj, J. (2017). Theory of triangular fuzzy number. *Proceedings of NCATM*, 2017, 80.
- [29] Gani, A.N., Assarudeen, S.M. (2012). A new operation on triangular fuzzy number for solving fuzzy linear programming problem. *Applied Mathematical Sciences*, 6(11): 525-532.
- [30] Yen, K.K., Ghoshray, S., Roig, G. (1999). A linear regression model using triangular fuzzy number coefficients. *Fuzzy Sets and Systems*, 106(2): 167-177. [https://doi.org/10.1016/S0165-0114\(97\)00269-8](https://doi.org/10.1016/S0165-0114(97)00269-8)
- [31] Karimi, H., Sadeghi-Dastaki, M., Javan, M. (2020). A fully fuzzy best-worst multi attribute decision making

- method with triangular fuzzy number: A case study of maintenance assessment in the hospitals. *Applied Soft Computing*, 86: 10588. <https://doi.org/10.1016/j.asoc.2019.105882>
- [32] Xie, Z., Su, Z. (2021). Evaluation of college English classroom teaching quality dependent on triangular fuzzy number. *The International Journal of Electrical Engineering & Education*, 00207209211002075. <https://doi.org/10.1177/00207209211002075>
- [33] Roy, A., Singha, J., Laskar, R.H. (2018). Removal of impulse noise from gray images using fuzzy SVM based histogram fuzzy filter. *Journal of Circuits, Systems and Computers*, 27(09): 1850139. <https://doi.org/10.1142/S0218126618501396>
- [34] Kumar, S.V., Nagaraju, C. (2018). Fuzzy entropy based impulse noise detection and correction method for digital images. *International Journal of Image, Graphics and Signal Processing*, 12(3): 36. <https://doi.org/10.5815/ijigsp.2018.03.05>
- [35] Roy, A., Manam, L., Laskar, R.H. (2018). Region adaptive fuzzy filter: an approach for removal of random-valued impulse noise. *IEEE Transactions on Industrial Electronics*, 65(9): 7268-7278. <https://doi.org/10.1109/TIE.2018.2793225>
- [36] Kiani, V., Zohrevand, A. (2019). A fuzzy directional median filter for fixed-value impulse noise removal. In 2019 7th Iranian Joint Congress on Fuzzy and Intelligent Systems (CFIS), pp. 1-4. <https://doi.org/10.1109/CFIS.2019.8692165>
- [37] Schulte, S., Nachtegael, M., De Witte, V., Van der Weken, D., Kerre, E.E. (2006). A fuzzy impulse noise detection and reduction method. *IEEE Transactions on Image Processing*, 15(5): 1153-1162. <https://doi.org/10.1109/TIP.2005.864179>
- [38] Yuksel, M.E., Besdok, E. (2004). A simple neuro-fuzzy impulse detector for efficient blur reduction of impulse noise removal operators for digital images. *IEEE Transactions on Fuzzy Systems*, 12(6): 854-865. <https://doi.org/10.1109/TFUZZ.2004.836075>
- [39] Russo, F., Ramponi, G. (1996). A fuzzy filter for images corrupted by impulse noise. *IEEE Signal Processing Letters*, 3(6): 168-170. <https://doi.org/10.1109/97.503279>
- [40] Schulte, S., De Witte, V., Nachtegael, M., Van der Weken, D., Kerre, E.E. (2006). Fuzzy two-step filter for impulse noise reduction from color images. *IEEE Transactions on Image Processing*, 15(11): 3567-3578. <https://doi.org/10.1109/TIP.2006.877494>
- [41] Verma, O.P., Singh, S. (2013). A fuzzy impulse noise filter based on boundary discriminative noise detection. *Journal of Information Processing Systems*, 9(1): 89-102. <https://doi.org/10.3745/JIPS.2013.9.1.089>
- [42] Morillas, S., Gregori, V., Hervás, A. (2009). Fuzzy peer groups for reducing mixed Gaussian-impulse noise from color images. *IEEE Transactions on Image Processing*, 18(7): 1452-1466. <https://doi.org/10.1109/TIP.2009.2019305>
- [43] Lin, T.C. (2011). Decision-based fuzzy image restoration for noise reduction based on evidence theory. *Expert systems with Applications*, 38(7): 8303-8310. <https://doi.org/10.1016/j.eswa.2011.01.016>
- [44] Wu, J., Tang, C. (2014). Random-valued impulse noise removal using fuzzy weighted non-local means. *Signal, Image and Video Processing*, 8(2): 349-355. <https://doi.org/10.1007/s11760-012-0297-1>
- [45] Chen, Y., Zhang, Y., Shu, H., Yang, J., Luo, L., Coatrieux, J.L., Feng, Q. (2016). Structure-adaptive fuzzy estimation for random-valued impulse noise suppression. *IEEE Transactions on Circuits and Systems for Video Technology*, 28(2): 414-427. <https://doi.org/10.1109/TCSVT.2016.2615444>
- [46] Wang, Y., Wang, J., Song, X., Han, L. (2016). An efficient adaptive fuzzy switching weighted mean filter for salt-and-pepper noise removal. *IEEE Signal Processing Letters*, 23(11): 1582-1586. <https://doi.org/10.1109/LSP.2016.2607785>
- [47] Roy, A., Singha, J., Devi, S.S., Laskar, R.H. (2016). Impulse noise removal using SVM classification based fuzzy filter from gray scale images. *Signal Processing*, 128: 262-273. <https://doi.org/10.1016/j.sigpro.2016.04.007>
- [48] Bandyopadhyay, A., Deb, K., Das, A., Bag, R. (2020). Impulse noise removal by k-means clustering identified fuzzy filter: A new approach. *Turkish Journal of Electrical Engineering & Computer Sciences*, 28(5): 2838-2862. <https://doi.org/10.3906/elk-1910-34>
- [49] Alaoui, N., Mashat, A., Adamou-Mitiche, A.B.H., Mitiche, L., Djalab, A., Daoudi, S., Bouhamla, L. (2021). Impulse noise removal based on hybrid genetic algorithm. *Traitement du Signal*, 38(4): 1245-1251. <https://doi.org/10.18280/ts.380436>